FAR-INFRARED ENERGY DISTRIBUTIONS OF ACTIVE GALAXIES IN THE LOCAL UNIVERSE AND BEYOND: FROM ISO TO HSO

Luigi Spinoglio[1], Paola Andreani[2], and Matthew A. Malkan[3]

[1]IFSI-CNR, Via Fosso del Cavaliere 100, I-00133 Roma, Italy
[2]Osservatorio Astronomico di Padova, Vicolo dell'Osservatorio, Padova, Italy
[3]UCLA Division of Astronomy & Astrophysics, Los Angeles, CA 90095-1562, USA

Abstract

New results of the ISO photometric survey of the 12 micron active galaxy sample are presented. We address issues on the far-infrared turnover and on the different overall shape of starburst and Seyfert type 1 and type 2 galaxies. These two latter types of active galaxies have far-IR energy distributions that can be indeed explained by different inclinations of an hypothetical obscuring torus.

The energy distributions of active and starburst galaxies in the Local Universe as measured by IRAS and ISO are then used to make predictions on what HSO will be able to achieve at significant redshifts. We have used the ISO photometric observations of active and starburst galaxies of the 12 micron galaxy sample to define average energy distributions of Seyfert type 1 and type 2, starburst and normal galaxies. Assuming different galaxy evolution laws, the derived energy distributions at various redshifts are then compared with the detection limits of the HSO camera arrays of PACS and SPIRE. Finally, from the mid-IR luminosity function of the Local Universe, we estimate the number of galaxies that HSO deep surveys will be able to detect.

Key words: Galaxies: evolution; active; starburst – Missions: ISO; HSO

1. Introduction

The 12μm galaxy sample (Spinoglio & Malkan 1989; Rush, Malkan & Spinoglio 1993) was selected to provide a complete and largely unbiased sample of local galaxies, not suffering the strong selection effects of optical-UV and far-IR surveys. The selection was done at 12μm because it was found that this band contains a constant fraction of bolometric flux for both active galaxies ($\sim$ 1/5) and normal galaxies ($\sim$ 1/14). It follows that 12μm selection is equivalent to select at a bolometric flux limit. In Figure 1 we show the energy distributions normalized to the bolometric flux for each galaxy class (Spinoglio et al. 1995).

We report here few of the results of ISOPHOT (Lemke et al. 1996) 120-150-170-180-200μm photometry on 39 galaxies, together with archive data on other 19 and literature data on 32 galaxies all belonging to the 12μm galaxy sample. The sample discussed here of 90 galaxies (29 Seyfert 1's, 35 Seyfert 2's, 12 high luminosity non-Seyfert's and 14 normal galaxies) is presently the largest sample of active galaxies in the Local Universe for which are available photometric data up to the wavelength of 200μm. The details of this study will be reported in a forthcoming article (Spinoglio, Andreani & Malkan 2000).

Based on ISO and IRAS results on these local galaxies, we make predictions on what luminosities and distances the HSO photometric arrays will be able to reach in a near future to study galaxy evolution.

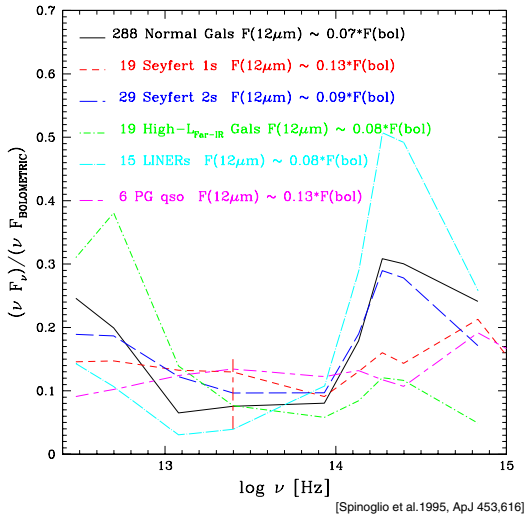

Figure 1. Energy distributions of galaxies of the 12μm sample normalized to the bolometric flux for the various classes. For each class the fraction of the bolometric flux contained in the 12 μm IRAS band is indicated.

2. Few ISO Results

2.1. Far-IR turnover versus 60μm excess

As shown in Figure 2, a correlation is found (P=92.5%) between the steepness of the far-IR turnover (measured from the [200-100] color) and the 60μm excess, which is an indicator of recent enhanced star formation. High-luminosity non-Seyfert galaxies (that mostly overlap with the optically classified starburst galaxies) are close to the ULIRGs (e.g. Arp220, Mk231, Mk273) which have strong 60μm ex-

Proc. Symposium *'The Promise of the Herschel Space Observatory'* 12–15 December 2000, Toledo, Spain
ESA SP-460, July 2001, eds. G.L. Pilbratt, J. Cernicharo, A.M. Heras, T. Prusti, & R. Harris

cess and low [200-100] color, lying in the upper right part of the diagram. On the contrary, most Seyfert galaxies not belonging to the CfA sample (Huchra & Burg 1992) have lower 60μm excess than the average, lying on the lower left part of the diagram, while only CfA Seyfert's lie above the correlation line, showing that they contain more galactic light emission and less nuclear emission than the other infrared selected Seyfert's.

We suggest that the diagram of the far-IR turnover versus the 60μm excess defines a region that we call *starburst dominated* above the correlation line, and another region *AGN dominated* below the line.

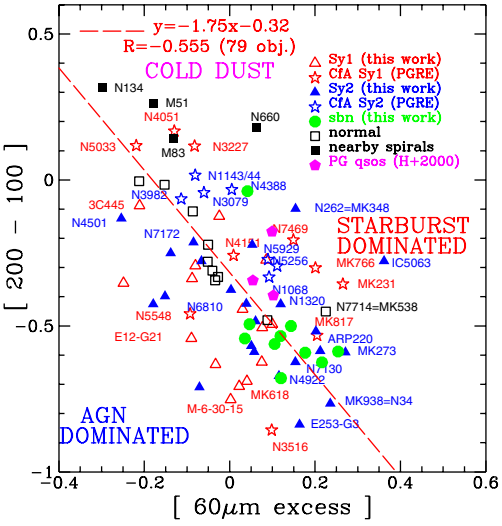

Figure 2. [200-100] color versus the 60μm excess for various types of galaxies, including the CfA Seyfert galaxies (Perez Garcia & Rodriguez Espinosa 2000) belonging to the 12μm sample. For comparison are also included the PG quasars (Haas et al. 2000).

2.2. Testing unified models of Seyfert 1's and 2's

Unified models claim that the observational differences between type 1 and type 2 Seyfert galaxies can be attributed to the different orientation of an hypothetical dusty torus. To qualitatively test this hypothesis, we have fitted in Figure 3 the average slope of the 12-200μm far-IR spectral energy distributions (SED) of Seyfert 1's and Seyfert 2's with the sum of an optically thick dusty torus seen face and edge on respectively, from the models by Granato & Danese (1994) and grey-body thermal emission at 25K with inverse square wavelength dependence of the dust emissivity. The sum of the torus emission and the cold dust thermal emission can roughly reproduce the observations.

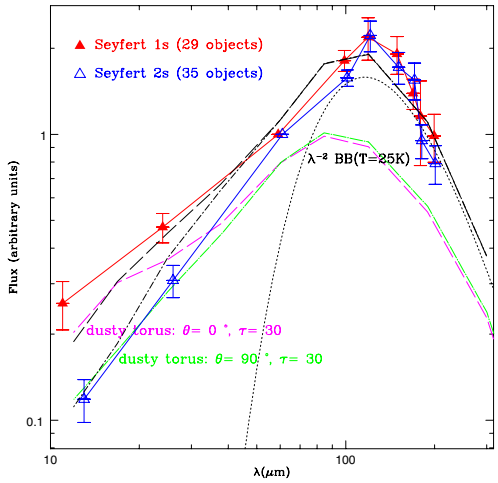

Figure 3. Comparison between the average Seyfert 1's (red triangles) and 2's (blue triangles) energy distributions. The green line shows the edge on model ($\theta = 90°$, $\tau = 30$); the pink line the face on model $\theta = 0°$, $\tau = 30$) from Granato & Danese (1994); the dotted line grey-body emission at T=25K.

2.3. Energy distributions from 0.44 to 200μm

In Figure 4, we show the SED of the different classes of galaxies normalized to 12μm. Seyfert 1's have the flatter SED, showing the larger power at 0.44 and 3.6μm. Seyfert 2's show two peaks: at 100μm and 1.6μm. High luminosity non-Seyfert's show the brightest peaks at 100μm and the weakest one at 1.6μm. Normal galaxies show again two peaks: at 100μm and 1.6μm.

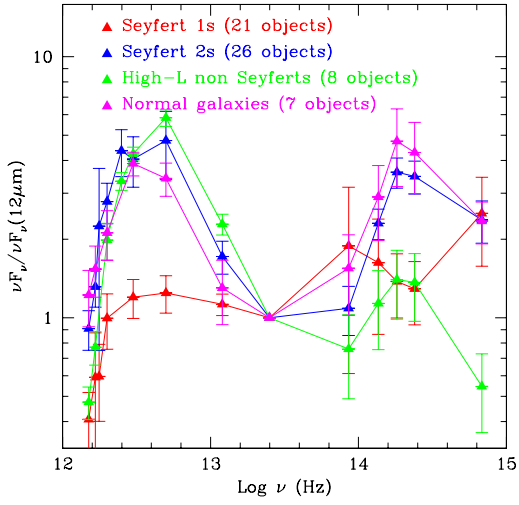

Figure 4. Combined energy distributions of active and normal galaxies of the 12μm sample from 4400Å to 200μm.

3. What luminosities will HSO detect?

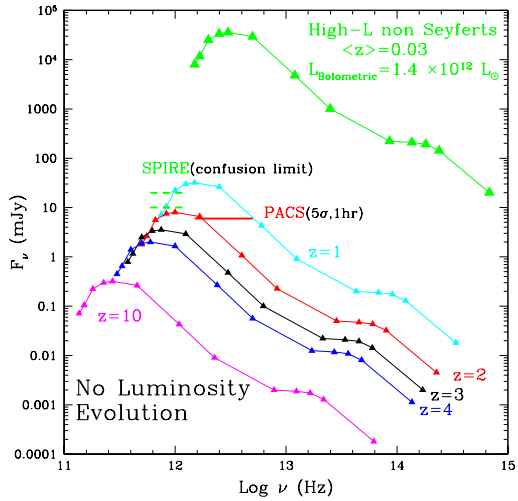

Figure 5. Without luminosity evolution a galaxy of $L = 1.4 \times 10^{12} L_{\odot}$ *can be detected: by PACS in 1 hr at* $\sim 50\,\sigma$ *at z=1 and at* $\sim 5\sigma$ *at z=2; by SPIRE above the confusion limit (assumed in the range* $10 - 20 mJy$*) only at z=1.*

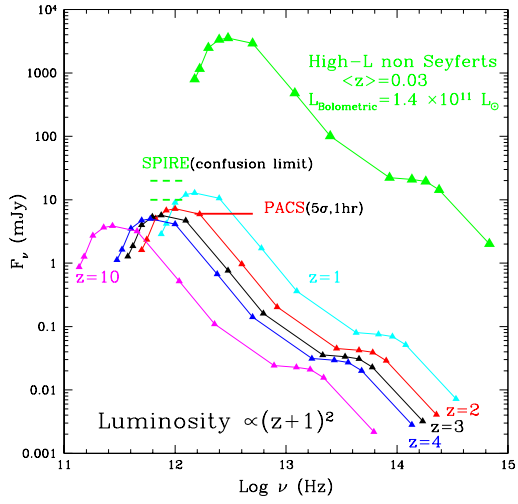

Figure 6. With the $L(z) \propto (z+1)^2$ *evolution : a galaxy of* $L = 1.4 \times 10^{11} L_{\odot}$ *can be detected: by PACS in 1 hr at* $\sim$ *10* σ *at z=1 and at* $\sim 5\sigma$ *at z=2; by SPIRE above the confusion limit only at z=1.*

From the analysis of the local 12μm galaxy sample we have derived the following relations between bolometric flux and 12μm flux:

- Seyfert type 1: $F_{12\mu m} \sim 0.13 F_{BOL}$
- Seyfert type 2: $F_{12\mu m} \sim 0.09 F_{BOL}$

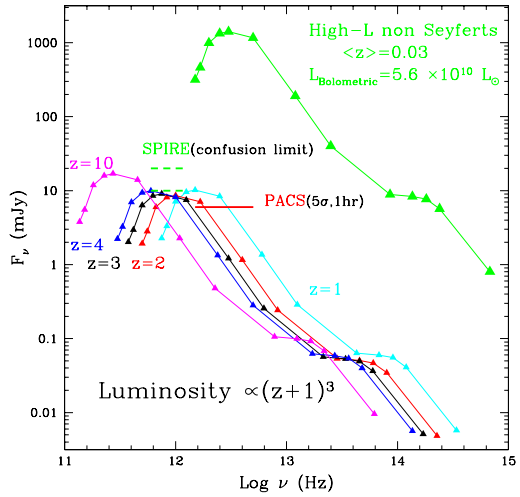

Figure 7. With the strong evolution $L(z) \propto (z+1)^3$ *a galaxy of* $L = 5.6 \times 10^{10} L_{\odot}$ *can be detected: by PACS in 1 hr at* $\sim 10\sigma$ *at any z; by SPIRE above the confusion limit at any z.*

- High Luminosity non Seyfert's : $F_{12\mu m} \sim 0.08 F_{BOL}$ (starburst galaxies)
- Normal galaxies: $F_{12\mu m} \sim 0.07 F_{BOL}$

If we want to focus on the non-AGN population of the high-luminosity non-Seyfert's (defined as having $L_{FIR} > 1.6 \times 10^{11} L_{\odot}$) (corresponding to the starburst population) and make predictions on their observability with HSO, we can use the same relation:

$$L_{BOL} \sim 4\pi D^2 (1/0.08) F_{12\mu m} \nu_{12\mu m} \times E(z)$$

where E(z) indicates the redshift dependence of the assumed luminosity evolution. For different evolutionary models we computed the luminosities that we can detect with the photometer arrays of PACS and SPIRE on board of HSO. Figure 5, 6 and 7 show the flux distribution that an high luminosity non-Seyfert galaxy of a given luminosity in the Local Universe would have at different redshifts, assuming different luminosity evolution laws.

4. How many galaxies will HSO detect ?

Taking the Local Luminosity Function e.g. at 12μm (Rush, Malkan & Spinoglio 1993; Fang et al. 1998; Xu et al. 1998), we can derive how many galaxies HSO will see at redshift of 1 and 2, by adopting an evolutionary model. Following the review by Franceschini (2000), ISO deep counts can be interpreted as due to the combination of two source populations : a non-evolving and a strongly evolving one. Two models are considered for the strong evolving population:

$$n[L(z), z] = n_o(L_o) \times (1+z)^{4.5} \qquad L(z) = L_o \times (1+z)^2 \quad (A)$$

$$n[L(z), z] = n_o(L_o) \times (1+z)^{6} \qquad L(z) = L_o \times (1+z)^3 \quad (B)$$

We report in Table 1 the space density of evolving galaxies derived from the 12μm luminosity function of

Fang et al. (1998), assuming that the evolving population is 10% of the total, and the two evolution laws of models A and B. Finally in Table 2, we give the differential number of galaxies per unit magnitude for the typical size of a deep survey ($1^\circ \times 1^\circ$) in a slice of $\Delta z = 1.0$ centered at z=1 and z=2.

Table 1. Space density of galaxies ϕ $[Mpc^{-3}(mag)^{-1}]$, assuming that the evolving population is 10% of the total, compared to the local luminosity function (LF) (Fang et al. 1998)

Luminosity (at z=0) ($L_\odot$)	Local LF	z	Model A	Model B
$10^{10.2}$	6.3×10^{-5}		1.4×10^{-4}	4.0×10^{-4}
10^{11}	7.8×10^{-7}		1.8×10^{-6}	5.0×10^{-6}
$10^{12.2}$	1.3×10^{-9}		2.9×10^{-9}	8.3×10^{-9}
$10^{10.2}$	6.3×10^{-5}		8.8×10^{-4}	4.6×10^{-3}
10^{11}	7.8×10^{-7}		1.1×10^{-5}	5.7×10^{-5}
$10^{12.2}$	1.3×10^{-9}		1.8×10^{-8}	9.5×10^{-8}

Table 2. Differential Number of galaxies in $1^\circ \times 1^\circ$ corresponding to 600 PACS beams (=112.5 SPIRE beams)

Area	z	Luminosity (at z=0) ($L_\odot$)	Model A	Model B
$1^\circ \times 1^\circ$	1	$10^{10.2}$	301	860
		10^{11}	3.9	10.7
		$10^{12.2}$	6.2×10^{-3}	1.8×10^{-2}
$1^\circ \times 1^\circ$	2	$10^{10.2}$	1,927	10,074
		10^{11}	24.1	124.8
		$10^{12.2}$	3.9×10^{-2}	2.1×10^{-1}

5. Conclusions

The study of the local population of active and starburst galaxies is a fundamental issue to understand the results (from ISO, JCMT and COBE) at significant redshift.

In local galaxies, the steepness of the FAR-IR turnover (measured by the [200-100] color) anti-correlates with the 60μm excess, showing that a large content of cold dust cannot survive during enhanced star formation.

In local galaxies the [200-100] color anti-correlates with redshift and luminosity, showing that more luminous objects are warmer.

The HSO photometer arrays will be able to detect galaxies as weak as $L = 0.5 - 1.4 \times 10^{11} L_\odot$ at z=1 and z=2 if these galaxies are evolving in luminosity as $L \propto (z+1)^2$ and at any redshift if there is the strong evolution $L \propto (z+1)^3$; if no evolution is present, still galaxies as weak as $L = 1.4 \times 10^{12} L_\odot$ at z=1 can be detected.

Density evolution -if existent- will also greatly help in the detection of distant galaxies.

Acknowledgements

The authors are grateful to the LWS Consortium and the ISO Staff at VILSPA (Villafranca, Spain) for the work done for building and operating, respectively, the Long Wavelength Spectrometer (LWS) onboard ISO. This research was funded in Italy by the Italian Space Agency (ASI).

References

Granato G.L., Danese L. 1994, MNRAS 268, 235
Fang F., Shupe D.L., Xu C., Hacking P.B. 1998 ApJ 500, 693
Fanti C. et al. 2000, A&A 358, 499
Franceschini, A. 2000, To appear in "Galaxies at High Redshift", I. Perez-Fournon, M. Balcells, F. Moreno-Insertis and F. Sanchez Eds., Cambridge University Press, astro-ph/0009121
Haas, M., et al. 2000, A&A 354, 453
Huchra J. & Burg R. 1992, ApJ 393, 90
Lemke D. et al. 1996, A&A 315, L64
Pérez García A.M. & Rodríguez Espinosa J. M. 2000, astro-ph/0003349
Rush B., Malkan M.A. & Spinoglio L. 1993, ApJSS 89,1
Spinoglio L. & Malkan M.A. 1989, ApJ 342, 83
Spinoglio L. et al. 1995, ApJ 453, 616.
Spinoglio L., Andreani, P. & Malkan M.A. 2000, in preparation.
van Bemmel I. M., Barthel P. D. de Graauw T. 2000, A&A 359, 523
Xu C. et al. 1998, ApJ 508, 576